Published in final edited form as:
Mol Reprod Dev. 2011 ; 78(10-11): 868–878. doi:10.1002/mrd.21373.

The Echinoid Mitotic Gradient: Effect of Cell Size on the Micromere Cleavage Cycle

Rosalie E. Langelan Duncan[*] and **Arthur H. Whiteley**[†]
Department of Biology and the Friday Harbor Laboratories, University of Washington, Seattle, Washington

SUMMARY

Like other euechinoids, the fertilized eggs of the sand dollar *Dendraster excentricus* proceed through cleavages that produce a pattern of macromeres, mesomeres, and micromeres at the 4th division. The 8 cells of the macro-mesomere lineage proceed through 6 additional cleavages before hatching. At the fifth overall division, the 4 micromeres produce a lineage of large micromeres that will divide 3 additional times, and a lineage of small micromeres that will divide once more before hatching. Irrespective of lineage, the length of the cell cycles is closely related to the size of the blastomere; cells of the same size have the same cell cycle time. A consequence is that at the fourth cleavage, there is a gradient of mitotic activity from the fastest dividers at the animal pole and the slowest cleacing micromeres at the vegetal pole. By the time of hatching, which is the 10th division of meso-macromeres, all cells are the same small size, the metachronic pattern of division gives way to asynchrony, and the mitotic gradient along the polar axis is lost. Experimental pre-exposure to sodium dodecyl sulfate (SDS), however, blocks the appearance of the gradients in cell size, the mitotic gradient, and the differential in cell cycle times. It is proposed that the mitotic gradients, cell cycle times, and attainment of a state of asynchrony are functions of cell size. Developmental consequences of the transition are large, and include coordinated activation of transcriptions, synthesis of new patterns of proteins, alterations of metabolism, and onset of morphogenesis.

Keywords

sand dollar; mitotic metachrony; micromere; nucleo-cytoplasmic ratio

INTRODUCTION

The 5th cell cycle of sea urchin embryos represents a transition stage from mitotic synchrony to a period of relative mitotic activity. The first four cleavages of sea urchin embryos are synchronous and are characterized by an absence of both G_1 and G_2 phases during the cell cycle, whereas the subsequent cleavages are characterized both by the introduction of G_1 and G_2 phases (Dan et al., 1980) and by a gradient of mitotic activity extending from the vegetal pole to the animal pole (Agrell, 1956; Parisi et al., 1978).

The loss of mitotic synchrony coincides with an unequal cleavage that forms micromeres at the vegetal pole. The micromeres have a slow cleavage cycle whereas the macromeres and mesomeres may remain synchronized up to the 7th division in some species (Zeuthen, 1951; Agrell, 1956; Hagstrom and Lonning, 1964, 1965; Masuda, 1979; Dan et al., 1980). Gradually, vegetal blastomeres advance in division relative to those in the animal

[†]corresponding author address: The Friday Harbor Laboratories, 620 University Road, Friday Harbor, WA 98250.
[*]current address: 6159 Old Brentford Court, Alexandria VA 22310

hemisphere, thus the micromeres have been proposed to act as pacemaker cells for this mitotic gradient (Parisi et al., 1978).

Masuda and Sato (1984) defined the cleavage period containing the mitotic gradient as metachronous rather than asynchronous. They demonstrated that the onset of true asynchrony occurs coincidentally with ciliogenesis after the 9th cleavage in *Hemicentrotus pulcherrimus*. Thus there are two transitions in cell cycle regulation during sea urchin cleavage: (1) synchrony to metachrony at the onset at 5th cleavage, and (2) metachrony to asynchrony at ciliogenesis (Masuda and Sato, 1984). By the time of hatching at the blastula stage, the echinoid embryo has undergone 9–10 divisions, depending on species, and the mitotic index falls dramatically (Parisi et al., 1978; Easton and Whiteley, 1979; Masuda and Sato, 1984).

The transition from synchronous to asynchronous divisions is one of great developmental consequence, as lengthening cell cycles coincide with transcriptional activation (Edgar et al., 1986) that may be cell- and stage-specific (Harkey, Whiteley and Whiteley, 1988 and 1992). Regulation of the mitotic gradient and the initiation of asynchrony in sea urchins have not been explained, however. Nucleo-cytoplasmic ratio has been shown to affect the onset of asynchrony in cleaving blastomeres of a number of developmental systems (Newport and Kirschner, 1982 a, b; Mita, 1983; Edgar et al., 1986). Experiments with haploid sea urchin embryos and egg fragments demonstrated that the first five cycles are independent of cell volume and ploidy, but such studies examined neither the mitotic gradient nor the onset of asynchrony in sea urchins (Harvey, 1956; Rustad, 1969).

The sea urchin embryo has two unequal divisions that change cell volumes among the cell types: the 4th, which produces micromeres, macromeres and mesomeres; and the 5th during which each of the micromeres divides into a large micromere (LMi) and a small micromere (SMi). It is conceivable, therefore, that the mitotic gradient reflects differences in nucleo-cytoplasmic ratio. To examine the influence of cell size on the timing of the transition from synchrony to metachrony at the 5th cleavage, we observed the cleavage and mitotic cycles of *Dendraster excentricus* sand dollar embryos in control conditions, and compared these with cell cycles in embryos in which the 4th and 5th cleavages were experimentally manipulated to produce blastomeres of the same size, thus abolishing the formation of micromeres as such. The results suggest that both the mitotic gradient along the polar axis and the onset of asynchrony may be regulated as a function of cell size in echinoid embryos.

RESULTS

The Mitotic Gradient

In embryos of the euechinoid subclass, including the modern sea urchins and sand dollars, the 5th cleavage divides the 4 micromeres into two tiers of unequally sized cells: 4 large, outer micromeres (large micromeres, LMi) and 4 small, inner micromeres (small micromeres, SMi) at the vegetal pole. The pattern of mitoses in these cells was observed in Feulgen-stained whole mounts embryos of the sand dollar *D. excentricus*. Mitotic synchrony disappeared at the 5th mitosis, in which the micromeres lagged slightly behind the other blastomeres the start of the period of metachrony. At the next division, the micromeres displayed distinctive long cell cycles, i.e., they remained in interphase while the macromeres and mesomeres proceeded synchronously through it (Fig. 1a). At the next LMi division (6th overall), spindles were oriented to produce a ring of 8 cells surrounding 4 SMi that remained in interphase (Fig. 1b). Because of the slow division cycle of the SMi, *D. excentricus* embryos did not pass through a 64-cell stage but produced a 60-cell stage instead. This pattern also has been observed in the sand dollar *Echinocyamus pusillus*. On the basis of this

delayed micromere division, Hagstrom and Lonning (1965) described 7 cleavage stages between 15-cell and 216-cell embryos.

The metachronous mitotic wave was pronounced at the 7th division. A normal embryo at the 7th mitosis (Fig. 1c) displayed, from the animal to the vegetal pole, the mesomeres in metaphase and the macromeres in anaphase of the 7th mitosis; 8 LMi in the preceding interphase; and SMi, numbering only 4, in interphase prior to their 6th division. This pattern of mitosis, with the macromeres leading, the mesomeres intermediate, and the micromeres following in two shifts, is termed the mitotic gradient (Agrell, 1956; Parisi et al., 1978). The gradient persisted at the 8th and 9th divisions (Fig. 1e). The orientation of embryos could be discerned by the presence of a cluster of compact micromere nuclei at the vegetal pole.

Nuclei of the SMi divided following the 7th macromere division (Fig. 2). There have been several reports that the SMi become haploid (Lindahl, 1953, Agrell, 1956), but in *D. excentricus* no chromosome loss was observed at the 5th overall mitosis that produced the SMi (Fig. 2a) or at the next division; SMi undergo their first mitosis (6th overall) normally. Divisions of the SMi could not be distinguished during later embryogenesis using this method.

To examine the mitotic gradient in embryos with equal cleavage, the embryos were first treated with sodium dodecyl sulfate (SDS) at the 4-cell stage and then returned to seawater. This treatment prevented micromere formation at the 4th cleavage, and the mitotic gradient was eliminated in these embryos. Although it was difficult to identify the animal-vegetal axis solely by the orientation of metaphases in preparations in which all cells were of a uniform size and all nuclei were synchronized, all 32 blastomeres of SDS-equalized embryos progressed through the 6th mitosis synchronously (Fig. 3a). Similarly, the synchrony of mitosis at the 7th division in SDS-equalized embryos was almost complete and no gradient pattern was detected (Fig. 3b). By the 8th division, however, asynchrony was observed in some embryos in which a group of small cells exhibited a delay in mitosis (Fig. 3c). These small cells may be the result of an additional, unequal division at the vegetal pole of SDS-equalized *D. excentricus* embryos (Langelan and Whiteley, 1985). The degree of synchronization was variable in cultures equalized by SDS treatment, but equalized embryos reproducibly exhibited increased synchrony at the 5th, 6th, and 7th divisions, and a corresponding slight increase in cell number as the micromere lineage proliferated in synchrony with the rest of the embryo. These results correspond with those reported for *Paracentrotus lividus* (Filosa et al., 1985).

Cell Cycle Length

The cleavage divisions of vegetal blastomeres were observed with time-lapse video microscopy to determine the behavior of micromeres and to measure cell cycles in normal (control) and SDS-equalized embryos. The relative cell cycles of macromeres and micromeres were observed; mesomeres usually were out of the plane of focus, and therefore excluded from the field of view.

In general, the time-lapse recording confirmed the patterns observed in Feulgen-stained embryos. Control, 16-cell stage micromeres lagged slightly behind the macromeres in both nuclear membrane breakdown and cytokinesis at the unequal 5th division (Fig. 4a, b) giving rise to the 32-cell stage embryo containing 4 LMi and 4 SMi at the vegetal pole (Fig. 4c). At the ensuing division (6th overall), all micromeres lagged in nuclear membrane breakdown and in completion of cytokinesis compared to the macromeres (Fig. 4d–f). At the macromere 7th division, both LMi and SMi again lagged (Fig. 4g).

The 4 SMi (14–17 μm diameter) exhibited a very long 6th cell cycle such that their 2nd division occurred after the 7th cleavage of the macromeres (Fig. 4h). Only two out of 18 SMi progeny were observed to undergo an additional cleavage prior to ciliation of the rest of the embryo. The micromere population of 24 cells (16 LMi and 8 SMi) remained in interphase at the macromere 8th division (Fig. 4i). Ciliation of the embryos occurred after the macromere 9th cleavage and LMi 8th cleavage. Cleavages were not followed beyond the time of ciliation.

The SMi exhibited pulsatory behavior that was pronounced in the time-lapse recordings. They usually sat on top of the epithelium at the 60-cell stage (above the plane of view in Fig. 4e), and repeatedly extended broad protrusions that withdrew and changed location within minutes. The active behavior of this cell type was observed in the SMi and in their progeny. The irregular shape of the SMi progeny in Fig. 4i gives some indication of this behavior. In contrast to reports by Hagstrom and Lonning, (1965), no connections were observed among micromeres or macromeres during cleavage. In unpublished electron microscope images of 16-cell stage embryos of *Strongylocentrotus purpuratus*, one of us (RLD) has observed junctional complex-like thickenings between mesomeres and macromeres, and between macromeres and micromeres.

Embryos equalized by brief SDS-treatment at the 4-cell stage displayed a cleavage schedule different from that of controls. An embryo completely equalized by the SDS-treatment showed equal and synchronous cleavages at the vegetal pole (Fig. 5). The orientation of this embryo was identified as a 3-tiered embryo (Langelan and Whiteley, 1985, their Fig. 7), i.e. with a tier of 4 cells at the vegetal pole (Fig. 5a), another tier of 4 cells at a deeper focus and 8 cells, still deeper, at the animal pole. At the 5th and 6th cleavages, all vegetal pole blastomeres underwent nuclear membrane breakdown and cytokinesis within a few minutes of each other (Fig. 5b–d). Slight inequality in the 6th cleavage produced a single, smaller blastomere at the 64-cell stage (Fig. 5e, arrow). This smallest cell displayed the longest cell cycle, and was the last to undergo nuclear membrane breakdown for the 7th cleavage (Fig 5f). Likewise, a single, unequal 7th cleavage correlated with reduced synchrony at the 8th cleavage (Fig. 5g–i). In contrast to control micromeres, 7th, 8th, and 9th cleavages were observed in all vegetal blastomeres of this SDS-equalized embryo, even in cells of the micromere lineage.

SDS-treated embryos of the intermediate type, containing some micromeres and some equalized cells at the 16-cell stage, displayed normal, long cell cycles in the micromeres and shortened cell cycles in equalized cells within the same embryo (Fig. 6). This result indicates that SDS-treatment does not alter micromere cell cycle length independently of micromere size. Furthermore, control embryos with variation in micromere size showed a similar effect: unusually LMi had shorter cell cycles. On the basis of these observations, we conclude that long micromere cell cycles correlate with the small size of these micromeres.

Cell Volume and Cell Cycle

To examine the relationship between cell size and cell-cycle length during the metachronous period, we measured dimensions and cleavage times of individual blastomeres from their image on the video monitor. The temperature of these embryos was 17°C. The quadrants of the embryo (right/left') could not be identified, so lineage designations were based on labeling of the 32-cell stage embryo: macromeres, LMi and SMi. Because the cell cycles are different for these three lineages (macro-mesomere, LMi and SMi lineage), we used the following nomenclature for the three lineages after cleavage 4: MM 6, etc. for the macro-mesomere lineage in the 6th cell cycle, and LMi 1 or SMi 1 for the respective large or small micromere lineage in their first cell cycle.

Complete records of the metachronous period extending from 4th cleavage to 10th cleavage were obtained for the vegetal cells of 3 control and 3 experimental embryos. Table 1 presents these observations. The 6th cell cycle, for example, indicates the period between 5th and 6th cleavages. Control blastomeres showed a lengthening of cell cycle duration coincident with a reduction in cell diameter (Table 1). The macromeres of the vegetal layer were closely synchronized within each cycle. During the metachronous period, the average diameter of the macromere progeny decreased from 39.5 μm to 18.9 μm while the duration of the cycles increased almost two-fold (1–2/3), from 39.8 min at MM cycle 6, to 66.1 min at cycle 9 (Table 1, Macromeres). Ciliation was initiated after the 9th cleavage of the macromeres, followed by hatching during or after the 10th cleavage.

The LMi displayed a cleavage schedule similar to that of the macromeres (Table 1). The LMi cycle length increased from an average of 46.1 min at their cycle 1, to 133.5 min at their cycle 4, while their diameters diminished from 24.7 μm to 12.3 μm. Note that LMi of 19.1 μm diameter had long cell cycles similar to those of 18.9 μm diameter macromeres (58.3 min vs. 66.1 min).

Relatively few SMi were available for measurement, and variation among replicates was large and complicated by their pulsatory movement. None-theless, the length of cell cycles was longer for the small cells, and the values fall along the same trend lines as for LMi blastomeres.

SDS-equalized blastomeres also showed a lengthening of the cell cycle as cleavage proceeded (Table 1, SDS-Treated). The pattern paralleled that seen in control macromeres. Indeed cells in these SDS-treated embryos, which in controls would have been SMi, had undergone as many cleavages and had similar sizes and cycle durations as cycle-9 macromeres.

To statistically examine the relationship between cell volume and cell cycle length, the data of Table 1 were converted from diameter to volume using the formula for a sphere, and plotted on both linear and logarithmic scales. There is an inverse relationship between cell volume and cell cycle. The complete data sets for both normal and equalized embryos are summarized in Fig. 7. Standard linear regression performed on the log-log transformed data, and a statistical comparison of the slopes of the regression lines showed no significant difference between control and SDS-equalized embryos. Thus, there is an inverse relationship between cell volume and cell cycle length during the metachronous period irrespective of the cell lineage. This relationship extends to cells of pre-hatching embryos of about 1000 μm^3 volume or 12-μm diameter.

Cell Dissociation

Data obtained from time-lapse video suggested that blastomeres entered a very long cell cycle when they reached a diameter of 12–13 μm. To investigate the cell diameters of a population of control blastomeres as they progressed through cleavage to hatching after 10 cleavages, embryos were dissociated at each cleavage stage, and their blastomeres measured from photographs. These cultures were maintained at 11 °C in contrast to the time-lapse studies that were done at 17 °C. The results are shown in Fig. 8. The SMi, after their 6th division from fertilization, reached a diameter of 12.4 μm. The LMi underwent 8 divisions after fertilization, and reached a diameter of approximately 12 μm. The MM population of blastomeres underwent 10 cleavages, 6 more after the 4th cleavage. After hatching the entire population of blastomeres attained the diameter of 12 μm (Fig. 8). Since the cleavage cycles become asynchronous after hatching, these data suggest that a diameter of 12 μm represents a threshold limit for onset of asynchrony in *D. excentricus.*

DISCUSSION

The lengthening of cell cycles following 6th cleavage has been described in sea urchins (Dan et al., 1980; Masuda and Sato, 1984) and starfish (Dan-Sohkawa and Satoh, 1978). This observation is extended and quantified in the present study of the sand dollar. The large cells divided more quickly than the small cells, hence the macromeres cleaved faster than the mesomeres, which cleaved faster than the micromeres. During the metachronous period, cell cycle lengths increased in inverse correlation with cell volume in normal embryos. Equalization of 4th and 5th cleavages by treatment with SDS prevented micromere formation, enhanced the synchrony, and reduced the mitotic gradient of cleavage stage *D. excentricus* embryos. On the basis of these observations, we propose that cell cycle length from the 4th to 10th cleavages is regulated as a function of cell volume, and that the mitotic gradient established during this period is a result of unequal cell size.

An alternative explanation for the presence of the mitotic gradient, proposed by Parisi et al. (1978, 1979) and Filosa et al (1985), is that micromeres serve as pacemakers for the gradient, but a direct test of this idea, such as by transplantation of micromeres to another region of the embryo, has not been made. It is known that isolated macromeres and mesomeres cleave with the same schedule as in the intact embryo, and considerably faster than the micromeres (Hagstrom and Lonning, 1965), which is evidence that contact among the blastomeres is not rate-determining for cleavages.

Blastomeres during both the synchronous and the metachronous periods undergo division without detectable growth (cleavage-type cell cycles). The mechanisms controling cell cycle timing in cleavage-stage embryos is unclear (Yoneda and Schroeder, 1984). We propose that in the synchronous period preceding the 5th cleavage cytoplasmic, oscillators acting in all blastomeres synchronize the cell cycles. In the succeeding metachronous divisions, the resulting diminution of such oscillators by the decreasing nucleo-cytoplasmic ratio would account for the progressive slowing of cell cycles as cleavage proceeds. It is still unexplained why some blastomeres, e.g. the 4th cycle vegetal blastomeres, enter this period of slow growth and diminished size ahead of other cells.

The period of metachrony that begins at the fourth cleavage with the appearance of 4 micromeres ends at the time of hatching, which occurs at 22.5 hours in *Dendraster*. From the data of Figure 8, which is derived from the diameters of cells taken from a suspension at intervals during the cleavages, we have estimated the numbers of cells of the three lineages (SMi, LMi and MM) we would expect to be in the just-hatched embryo. Starting with the 4 micromeres of the 16-cell stage, two divisions produced 8 SMi blastomeres, and four divisions produced 32 LMi cell. Six divisions of the 12 macro-mesomeres of the 16-cell stage would potentially convert them into 768 cells, though these have not been specifically counted in *Dendraster*. Therefore at hatching at the 10th division after fertilization, there are about 808 cells. It is clear that at hatching, all of these cells have diameters of 12 μm (10.7–13.1). Subsequent divisions among the blastomeres are asynchronous.

A major shift in cell cycle regulation occurs coincident with hatching. It has been demonstrated that the mitotic index of echinoids decreases dramatically during the blastula stage, coincident with hatching (Parisi et al., 1978; Easton and Whiteley, 1979). Masuda and Sato (1984) reported the onset of asynchrony after the 9th division in *Temnopleurus toreumaticus* and demonstrated a sharp decrease in the cell cycle once the blastomeres become ciliated. In the present study, blastomeres of both control and SDS-equalized *D. excentricus* embryos achieved a diameter of 12 μm by the time of hatching. Thus in spite of unequal cleavages to produce micromeres, all cells attain the same size in the blastula due to the slow cleavage rate of the smallest cells. Some function of cell volume in the blastula

may regulate the transition to complete asynchrony around the time of hatching in sea urchins, as has been demonstrated in the vertebrate *Xenopus laevis* (Newport and Kirschner, 1982 a, b).

In support for this hypothesis, Mita (1983) demonstrated that half-sized egg fragments of the starfish *Asterina pectinifera* become asynchronous one cycle earlier than normal embryos. Studies of isolated sea urchin blastomeres and fused embryos show that cell number in sea urchin larvae can vary, whereas cell size is held constant (Morgan, 1895; Hörstadius, 1957; Takahashi and Okazaki, 1979. This is also true for dwarf larvae of *A. pectinifera* (Dan-Solkawa and Satoh, 1978).

After fertilization and throughout early cleavages until hatching, the echinoid embryo is undergoing events that will program it and determine important aspects of its development. Utilization of maternal transcripts and new transcription lead to the formation of regulatory networks involved in these crucial events (Oliveri et al., (2008). Yet, activation of many genes that contribute to differentiation and morphogenesis of the embryo are delayed until after hatching. After the 10^{th} cell cycle, with attainment of increased cell size, minimal nucleo-cytoplasmic ratio, and the end of metachrony, transcription of such genes occurs in both LMi and SMi. The normal fate of SMi includes production of the germline and probably other adult tissues, as first proposed by Tanaka and Dan (1990). A major role in regulating this expression is played by 3 *nanos* genes whose mRNAs accumulate in the 4 SMi as early as the 60-cell stage (Juliano et al., 2010). Their data suggests that the mRNAs of two of these genes maintains the SMi at the slow division rate, small size, and high nucleo-cytoplasmic ratio they had attained at the 4^{th} division. Juliano and colleagues found that if the transcription of these two genes is specifically inhibited after hatching, the SMi cell progeny at the tip of the archenteron of the gastrula make one additional, abnormal division, producing about 16 cells. Additionally the typical incorporation of these cells into the coelomic pouches fails, the larval echinus rudiment does not form, and metamorphosis fails. They suggest that these contributions of the SMi to the development of the rudiment may be both by direct genetic contribution to the tissues and by regulatory routes. A study of the regulation of activities of the LMi during this period would be of interest. In the LMi of *S. purpuratus*, a number of genes involved in skeletogenesis are totally quiescent until hatching and then, in a matter of minutes, are actively and coordinately expressed. In one of these transcriptions observed by *in situ* hybridization, the transcript is apparent in all 32 primary mesenchyme cells just as they emerge from the blastula wall into the blastocoel, and is absent from all other cells (Harkey et al., 1988, 1992). Whether this correlated activation of LMi genes is initiated by structural events related to cell-cell separation at ingression, to regulatory genes, or to other events is an open and interesting question. We do know that this precise, correlated activation of transcription of skeletogenic genes is coincident with the simultaneous achievement of minimal size by all blastomeres.

In addition to these and other transcriptional events, hatching and the onset of mitotic asynchrony in echinoids is followed directly by a number of other morphogenetic events and activities. These include (1) major changes in the pattern of protein synthesis (Harkey and Whiteley, 1983; Bedard and Brandhorst, 1983; Pittman and Ernst, 1984); (2) a switch in synthesis and utilization of histones (Ruderman and Gross, 1974; Easton and Whiteley, 1979); (3) changes in respiration (Borei, 1948; Gray, 1927; Whiteley and Baltzer, 1958; Immers and Runnstrom, 1960); (4) a shift in cell cycle regulation; and (5) transcriptional activity necessary for gastrulation (Giudice et al., 1968), among other developmental changes. Clearly, this post-hatching transition in echinoderms is comparable to the mid-blastula transition of *Xenopus laevis* embryos described by Newport and Kirschner (1982 a, b).

Thus, echinoid embryos, like those of other phyla, mark the end of cleavage with the onset of cell asynchrony, cell motility (ciliation in this case), and new gene transcription. The data reported here indicate that they also reach a threshold cytoplasmic volume, hence nucleo-cytoplasmic ratio, at this time. It is likely that the ratio between nuclear and cytoplasmic volume is a significant control mechanism for initiating embryonic transitions in a variety of eukaryotic embryos

MATERIALS AND METHODS

Gametes of *Dendraster excentricus* Escholtz were obtained by intracoelomic injection of 0.55 M KCl. Eggs were fertilized and cultured as monolayers in Falcon plastic petri dishes containing filtered seawater (FSW). The temperature varied from 9–12°C during the year, but was constant within an experiment, permitting good synchrony within the cultures. Normal, control embryos were cultured in FSW. To equalize embryos at the 4th cleavage, thus abolishing the normal distinction in cell volumes at the 16-cell stage, embryos were treated with 15–20 μg/ml sodium dodecyl sulfate (SDS; BDH, specially pure) in FSW for 40–45 min during the 4-cell stage, and returned to FSW for culture (Tanaka, 1975; Langelan and Whiteley, 1985).

The Mitotic Gradient

The mitotic gradient was visualized in Feulgen-stained whole mounts. All staining steps occurred at room temperature except where noted. One drop of FSW containing 50–100 embryos was placed on a subbed slide containing one drop of 45% acetic acid. After a minute, a coverslip was gently pressed over the preparation to compress the embryos. The coverslips were removed after freezing the preparations, and the embryos were fixed in 95% ethanol for 5 min and air-dried. After a rinse in distilled water, the slides were passed through 1N HCl for 2 min, 1N HCl at 60 °C for 1 min, 1N HCI for 1 min, and stained with Schiff's reagent for 60 min. They were rinsed once with SO_4 -saturated water, then three times with distilled water, dehydrated in tertiary butanol, and mounted in Permount. Some slides were counterstained with fast green in 70% ethanol during dehydration. The slides were examined with differential interference optics and photographed through a Nikon ND2 (T=50%) filter onto Technical Pan film (Kodak) using a Nikon Optiphot microscope.

Video Microscopy

Cell cycle lengths and cell diameters were measured from time-lapse video recordings of cleaving embryos. For video recording, a single drop of FSW containing 1 to 30 embryos at the 8- or 16-cell stage was placed on a glass microslide and covered by an 18 mm sq. #1 coverglass, supported at the corners by bits of modeling clay. The 4 edges of the coverslip were sealed to the slide with melted 1:1 paraffin-petrolium jelly. The drop of FSW containing the embryos was thus surrounded by air on 3 or 4 sides under the coverslip, but prevented from evaporation by the paraffin-vaseline seal.

The embryos were cooled by one of two methods during recording, but they were not perfused with flowing FSW. In the first method, the sealed slide containing the embryos was transferred to the underside of a brass-cooling chamber that permitted unimpeded observation at high resolution. The second cooling method was used during initial recordings. The slide containing embryos was cooled with a thermoelectric cooling stage (Cloney, Schaadt and Durden, 1970). A Tele-thermometer was used to measure the temperature on the coverslip directly in the light path at the end of the run. The recording temperature was approximately 17°C.

Initial time-lapse video recordings were made on a video system consisting of Dage MTI Newvicon camera, RCA time-date generator, Panasonic time-lapse VTR and Sony black-white monitor. Later recordings were made using a Gyyr time-lapse VCR and viewed with a Panasonic monitor.

A Plan 40X objective of a Zeiss differential interference microscope was used to record embryonic cleavages. The magnification was calibrated at the end of each sequence by recording a stage micrometer of 0.1 mm spacing. Cell diameter was measured with a transparent ruler placed directly on the image displayed on the video monitor. Two perpendicular diameters were measured for each cell, and these measurements were taken from nearly spherical cells whenever possible. The cells assumed a spherical shape directly after cleavage, but within 10 min settled back into an epithelium, assuming a polyhedral shape. If a spherical image of a particular cell was not available, average diameter was calculated from measurements of maximum and minimum diameters.

Cell cycle length was estimated as the time between consecutive cleavages. The time of cleavage was determined as the moment when furrowing was completed and detected as a relaxation of the cell. The videotaped images allowed simultaneous recording of cell diameter and cell cycle length in individual blastomeres.

Cell Dissociation

Gametes from a single female and male were used to establish a single culture for measuring blastomere sizes during cleavage. Fertilization membranes were removed 10 min after insemination by passing the culture through a 130-μm Nitex mesh immersed in FSW. This procedure stripped the fertilization membranes from 90% of the zygotes, which were then washed 2X with FSW and cultured as a monolayer in FSW at 11°C.

Embryos were dissociated using either of two different procedures, depending on their stage of development. The first procedure was designed to solubilize the hyaline layer from early cleavage stage embryos. De-membranated embryos from the 1-cell to the 256-cell stages were gently pelleted and washed once with ice-cold Bag isolation medium, pH 8.0, consisting of 40% dextrose, 40% calcium and magnesium-free artificial sea water, and 20% distilled water (Harkey and Whiteley, 1982). The embryos were resuspended in 0.2 ml Bag isolation medium and allowed to rest for 3–5 min on ice. Final separation was achieved by sucking the embryos into a pipette one time and expelling them back into Bag isolation medium, followed by preparation of a wet mount for photography. Cells were photographed in Bag isolation medium.

The second procedure was designed to dissociate early blastulae containing epithelial intercellular junctions. Embryos older than the 256-cell stage were removed from FSW by gentle hand centrifugation, washed 3X in ice-cold calcium and magnesium-free sea water, pH 8.0, and resuspended in 15 ml of dissociation medium, consisting of 0.1 M EDTA in 100 ml 1 M glycine, pH 8.0 (Harkey and Whiteley, 1982). The dissociated cells were pelleted by rigorous hand centrifugation and resuspended in dissociation medium. Efforts to return the cells to FSW usually resulted in cytolysis, therefore the cells were photographed in dissociation medium.

Photographs were taken of wet-mount preparations at each stage in order to measure cell diameters from prints using a magnified micrometer scale. Two perpendicular diameters were measured and averaged for each cell. One hundred cells were measured for each stage, but micromeres and their descendants were particularly sought to obtain as much data on the SMi population as possible.

Acknowledgments

Funding: NICHD Developmental Biology Training Grant, HD-07183

abbreviations

LMi	large Micromeres
MM	Meso-macromeres
SMi	Small micromeres
SDS	sodium dodecyl sulfate

References

Agrell, J. A mitotic gradient as the cause of the early differentiation in the sea urchin embryo. In: Wingstrand, KG., editor. Zoological Papers in Honor of B Hanstrom. 1956. p. 27-34.

Bedard PA, Brandhorst BP. Patterns of protein synthesis and metabolism during sea urchin embryogenesis. Devel Biol. 1983; 96:74–83. [PubMed: 6825961]

Borei H. Respiration of oocytes, unfertilized eggs and fertilized eggs from *Psammechinus* and *Asterias*. Biol Bull. 1948; 95:124–150. [PubMed: 18874958]

Cloney RA, Schaadt J, Durden JV. Thermoelectric cooling stage for the compound microscope. Acta Zool. 1970; 51:95–98.

Dan K, Tanaka S, Yamazaki K, Kato Y. Cell cycle study up to the time of hatching in the embryos of the sea urchin, *Hemicentrotus pulchierrimus*. Devel Growth Differ. 1980; 22:589–598.

Dan-Sohkawa M, Satoh N. Studies on dwarf larvae developed from isolated blastomeres of the starfish, *Asterina pectinifera*. J Embrvol Exp Morphol. 1978; 46:171–185.

Edgar BH, Kiehle C, Schubiger G. Cell cycle control by the nucleo-cytoplasmic ratio in early Drosophila development. Cell. 1986; 44:36172.

Easton DP, Whiteley AH. The relative contributions of newly synthesized and stored messages to H1 histone synthesis in interspecies hybrid echinoid embryos. Differentiation. 1979; 12:127–133. [PubMed: 467855]

Filosa S, Andreuccetti P, Parisi E, Monroy A. Effect on inhibition of micromere segregation on the mitotic pattern in the sea urchin embryo. Devel Growth Differ. 1985; 27:29–34.

Giudice G, Mutolo V, Donatuti G. Gene expression in sea urchin development. Wilhelm Roux Arch Entwicklungsmech Organ. 1968; 161:118.

Gray J. The mechanism of cell-division. II. Oxygen consumption during cleavage. Proc Camb Phil Soc (Biol Sri). 1925; 1:225–236.

Gray J. The mechanism of cell-division. III. The relationship between cell-division and growth in segmenting eggs. J Exp Biol. 1927; 4:313–321.

Hagstrom BE, Lonning S. The rate of development in isolated halves of sea urchin embryos. Sarsia. 1964; 15:17–22.

Hagstrom BE, Lonning S. Studies of cleavage and development of isolated sea urchin blastomeres. Sarsia. 1965; 18:1–9.

Harkey MA, Whiteley AH. Isolation, culture, and differentiation of echinoid primary mesenchyme cells. Wilhelm Roux' Arch. 1980; 189:111–122.

Harkey MH, Whiteley AH. The program of protein synthesis during the development of the micromere-primary mesenchyme cell line in the sea urchin embryo. Devel Biol. 1983; 100:12–28. [PubMed: 6617987]

Harkey MH, Whiteley HR, Whiteley AH. Coordinate accumulation of five transcripts in the primary mesenchyme during skeletogenesis in the sea urchin embryo. Devel Biol. 1988; 125:381–385. [PubMed: 2892749]

Harkey MH, Whiteley HR, Whiteley AH. Differential expression of the msp130 gene among skeletal lineage cells in the sea urchin embryo: a three dimensional in situ hybridization analysis. Mechanisms of Devel. 1992; 37:173–184.

Harvey, EB. The American Arbacia and Other Sea Urchins. Princeton Univ. Press; Princeton: 1956.

Hörstadius S. On the regulation of bilateral symmetry in plutei with exchanged meridional halves and in giant plutei. J Embryol Exp Morphol. 1957; 5:60–73.

Immers J, Runnstrom J. Release of respiratory control by 2, 4-dinitrophenol in different stages of sea urchin development. Devel Biol. 1960; 2:90–104. [PubMed: 13852759]

Juliano C, Yajima M, Wessel GM. *Nanos* functions ro maintain the fate of the small micromere lineage in the sea urchin embryo. Devel Biol. 2010; 337:220–232. [PubMed: 19878662]

Langelan RE, Whiteley AH. Unequal cleavage and the differentiation of echinoid primary mesenchyme. Devel Biol. 1985; 109:464–475. [PubMed: 3996759]

Lindahl E. On a normally occurring reduction-division in somatic cells of the sea urchin embryo. Exp Cell Res. 1953; 5:416. [PubMed: 13117009]

Masuda M, Sato H. Asynchronization of cell division is concurrently related with ciliogenesis in sea urchin blastulae. Devel Growth Differ. 1984; 26:281–294.

Mita I. Studies on factors affecting the timing of early morphogenetic events during starfish embryogenesis. J Exp Zool. 1983; 22:291–299.

Morgan TH. Studies of the 'partial' larvae of *Sphaerechinus*. Roux' Arch Ents Mech Organ. 1895; 2:81–126.

Newport J, Kirschner M. A major developmental transition in early *Xenopus* embryos: I. Characterization and timing of cellular changes at the midblastula stage. Cell. 1982a; 30:675–686. [PubMed: 6183003]

Newport J, Kirschner M. A major developmental transition in early *Xenopus* embryos: 11. Control of the onset of transcription. Cell. 1982b; 30:687–696. [PubMed: 7139712]

Oliveri P, Tu Q, Davidson E. Global regulatory logic for specification of an embryonic cell lineage. Proc Natl Acad Sci USA. 2008; 105:5955–5962. [PubMed: 18413610]

Parisi E, Rilosa S, DePetrocellis B, Monroy A. The pattern of cell division in the early development of the sea urchin, *Paracentrotus lividus*. Devel Biol. 1978; 65:38–49. [PubMed: 680360]

Pittman D, Ernst SG. Developmental time, cell lineage, and environment regulate the newly synthesized proteins in sea urchin embryos. Devel Biol. 1984; 106:236–242. [PubMed: 6489609]

Ruderman JV, Gross PR. Histones and histone synthesis in sea urchin development. Devel Biol. 1974; 36:286–298. [PubMed: 4814569]

Rustad RC. The independence of the mitotic rate of sea urchin eggs: from ploidy and cytoplasmic volume. Biophys Soc Abstr. 1969:A-186.

Takahashi MM, Okazaki K. Total cell number and number of the primary mesenchyme cells in whole, 1/2 and 1/4 larvae of *Clypeaster japonicas*. Devel Growth & Differ. 1979; 21:553–566.

Tanaka S, Dan K. Study of the lineage and cell cycle of small micromeres in embryos of the sea urchin, *Hemicentrotus pulcherrimus*. Devel Growth & Differ. 1990; 32:145–156.

Whiteley AH, Baltzer F. Development, respiratory rate and content of desoxyribonucleic acid in the hybrid *Paracentrotus* x *Arbacia*. Pubbl Staz Zool Napoli. 1958; 30:402–457.

Yoneda M, Schroeder TE. Cell cycle timing in colchicine-treated sea urchin eggs: Persistent coordination between the nuclear cycles and the rhythm of cortical stiffness. J Exp Zool. 1984; 231:367–378.

Zar, JH. Biostatistical Analysis. Prentice-Hall Inc; Englewood Cliffs, New Jersey: 1974.

Zeuthen E. Segmentation, nuclear growth and cytoplasmic storage in eggs of echinoderms and amphibia. Pubbl Staz Zool Napoli. 1991; 23(Suppl):47–69.

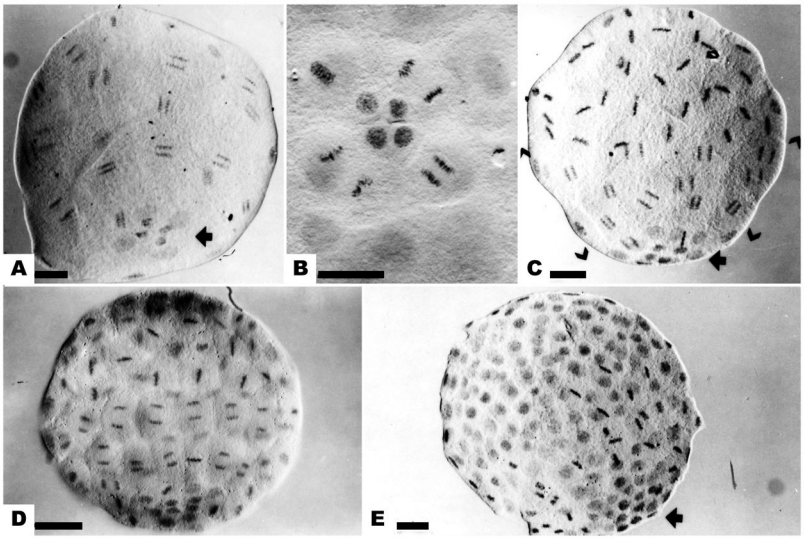

Figure 1.

The mitotic gradient in cleavage stage embryos of *Dendraster.* (a) Mesomeres and macromeres synchronized in anaphase of the sixth division. Four small micromeres (SMi) and 4 large micromeres (LMi) at the vegetal pole have not entered mitosis (arrow). (b) The 6^{th} division of the LMi. The SMi remain in interphase. (c) The 7^{th} division of the mesomeres and macromeres. The mesomeres are in metaphase, the macromeres in anaphase (brackets), and the micromeres in the preceding interphase. Four SMi at the vegetal pole have not divided (arrow). (d) The eighth division of mesomeres and macromeres, while LMi complete their 7^{th} division. (e) The ninth division of the macromeres, seen in metaphase. The micromeres can be identified as a group of small dense nuclei (arrow). Bar equals 25 μm.

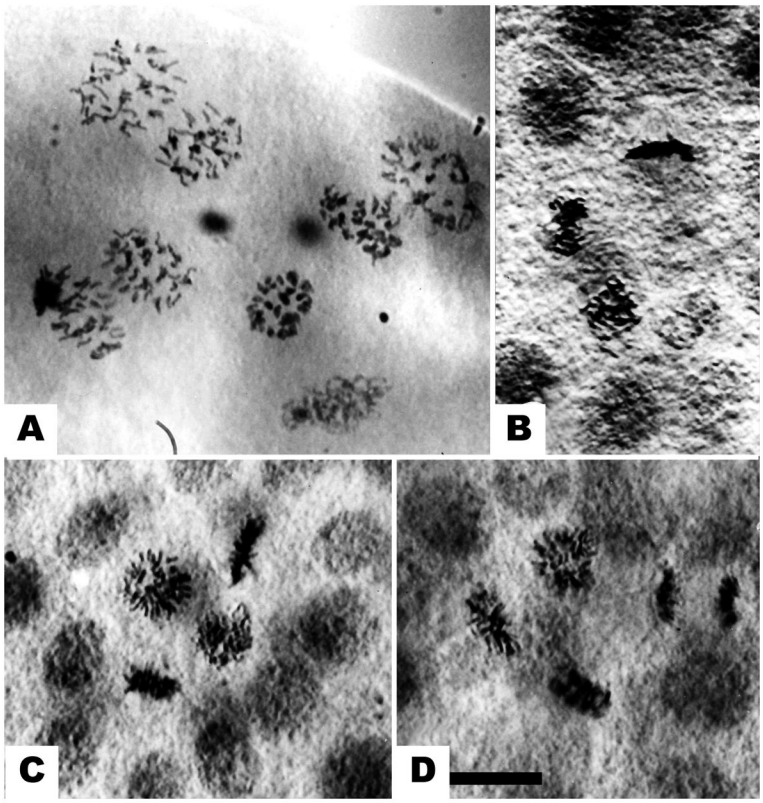

Figure 2.

Small micromere divisions. (a) The 5th division in the micromeres, shown at a face-on view of anaphase. Chromosomes of the 4 small micromeres (SMi) are in the center. No loss of chromosomes is evident. (b) The 6th division of the SMi, showing 2 cells in prophase, 1 in metaphase and 1 in telophase. (c) Another view of the SMi 6th division, showing chromosomes in 1 prophase and 3 in metaphases. (d). Same stage, showing 2 metaphases and 2 anaphases. Bar equals 10 μm.

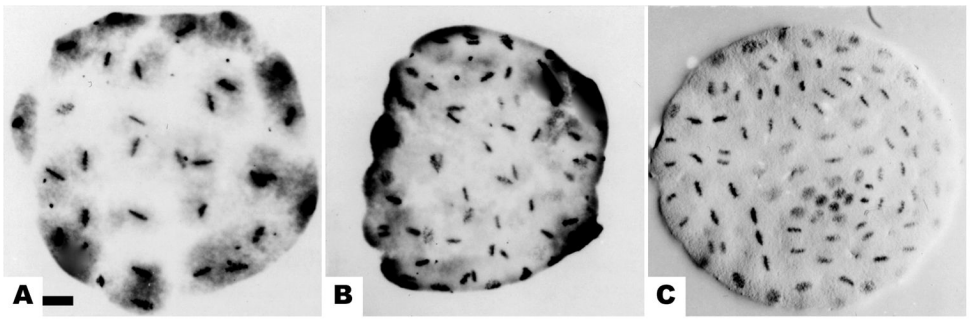

Figure 3.
Synchrony of mitotic stages in SDS-equalized *Dendraster* embryos. (a) All 32 blastomeres simultaneously in metaphase of 6th division. (b) All blastomeres in metaphase or prophase at the 7th division. (c) Surfactant-treated embryo at 8th cleavage showing group of small interphase nuclei, similar to control micromeres. Bar equals 25 μm.

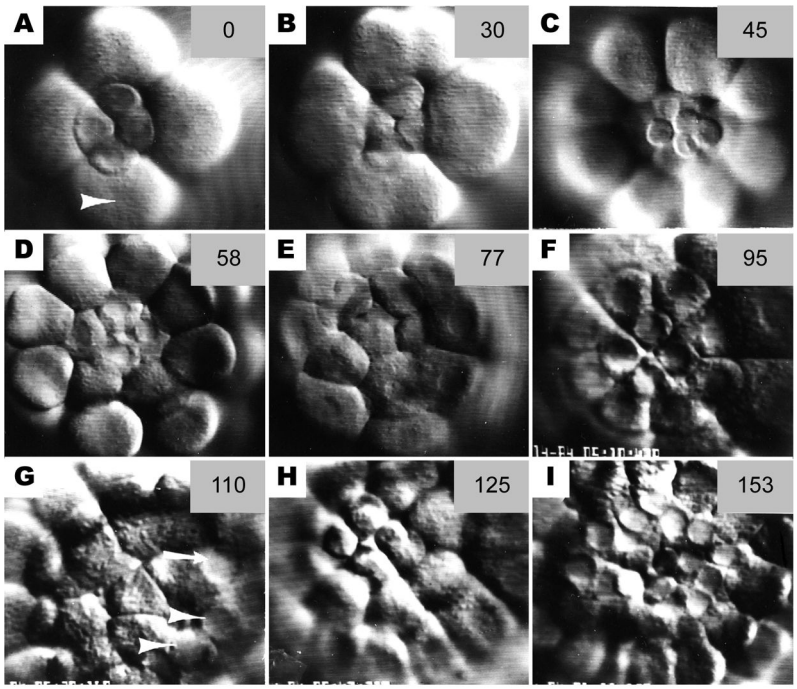

Figure 4.

Sequence of still photos from time-lapse video records of cleavage at the vegetal pole. (a) Late 16-cell stage. Micromere nuclei are intact whereas macromeres are beginning to furrow (arrowhead) (b) At the 5th cleavage, the micromeres have a slower cleavage schedule than the macromeres (c) The 32-cell stage, showing 4 small micromeres (SMi) atop 4 large micromeres (LMi); the 8 macromeres surround them. (d) The 4 LMi retain their nuclei while the macromeres undergo 6th cleavage. The SMi are above the plane or focus. (e) The 6th cleavage of the LMi. (f) The 60-cell stage showing 4 small and 8 LMi surrounded by the macromeres. (g) The 7th cleavage of the macromeres. Both small (arrowheads) and large (arrow) micromeres retain intact nuclei. Most micromere nuclei are not in focus in this photo, but all are intact. (h) The 6th cleavage of the SMi. LMi nuclei have broken down for the 7th cleavage. (i) The 8th cleavage of the macromeres. Note intact nuclei of the 24 micromeres. The numbers in the upper right of each frame are minutes elapsed from the first frames in the sequence at 17 °C.

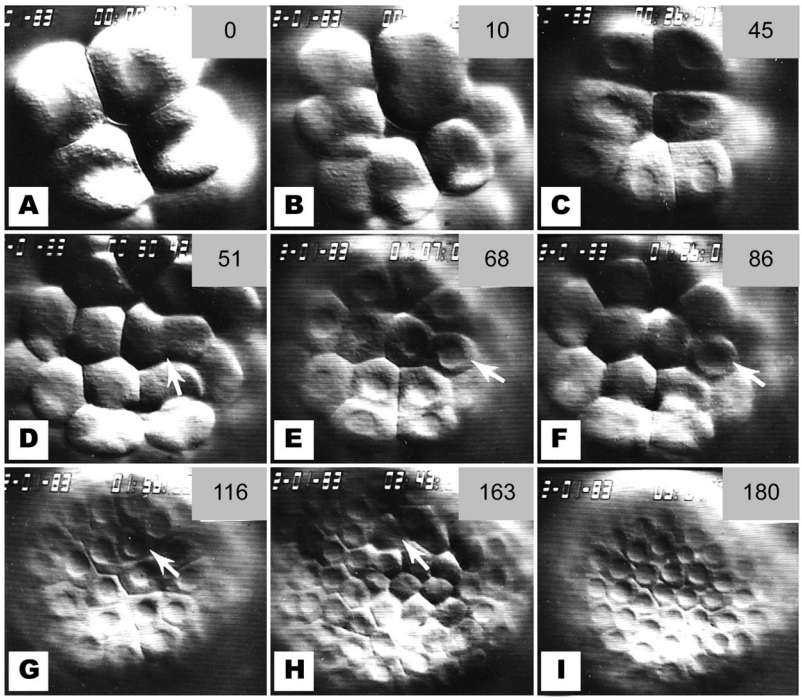

Figure 5.

Sequence of photos from SDS-treated, equalized embryo. Compare to Figure 4. (a) Vegetal pole at 16-cell stage, as identified by 4 blastomeres at this pole, 8 blastomeres at the opposite pole, and 4 blastomeres in the middle tier. (b) The 5th cleavage at the vegetal pole. (c) The 32-cell stage showing nuclei of the vegetal blastomeres. The cells identified by cleavage orientation as being of small micromere (SMi) lineage are pictured. (d) Synchronous 6th cleavage at the vegetal pole, in contrast to control embryos. One cleavage furrow is slightly eccentric (arrow). (e) The 64-cell stage, a stage not achieved by control embryos. Note the single smaller blastomere (arrow). (f) Nuclear membrane breakdown for the 7th cleavage. The smaller blastomere is the last to undergo nuclear membrane breakdown (arrow). (g) The 128-cell stage. Another unequal cleavage produced a small blastomere (arrow). (h) This small blastomere (arrow) is the last to divide at 8th cleavage. (i) The vegetal pole at the 256-cell stage of this equalized embryo. Compare to Figure 4i.

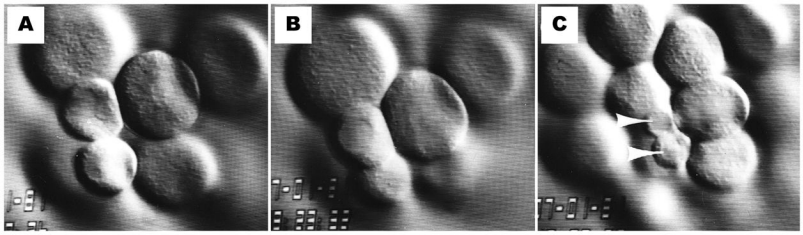

Figure 6.
The 5th division of an SDS-treated embryo with an intermediate cleavage pattern. (a) A 16-cell stage embryo with 2 micromeres and 2 equalized cells. (b) Nuclear membrane breakdown for 5th cleavage occurs earlier in the equalized cells than in the micromeres. (c) The 32-cell stage. The 2 small micromeres (SMi) are the last to undergo nuclear membrane breakdown for 6th cleavage (arrowheads).

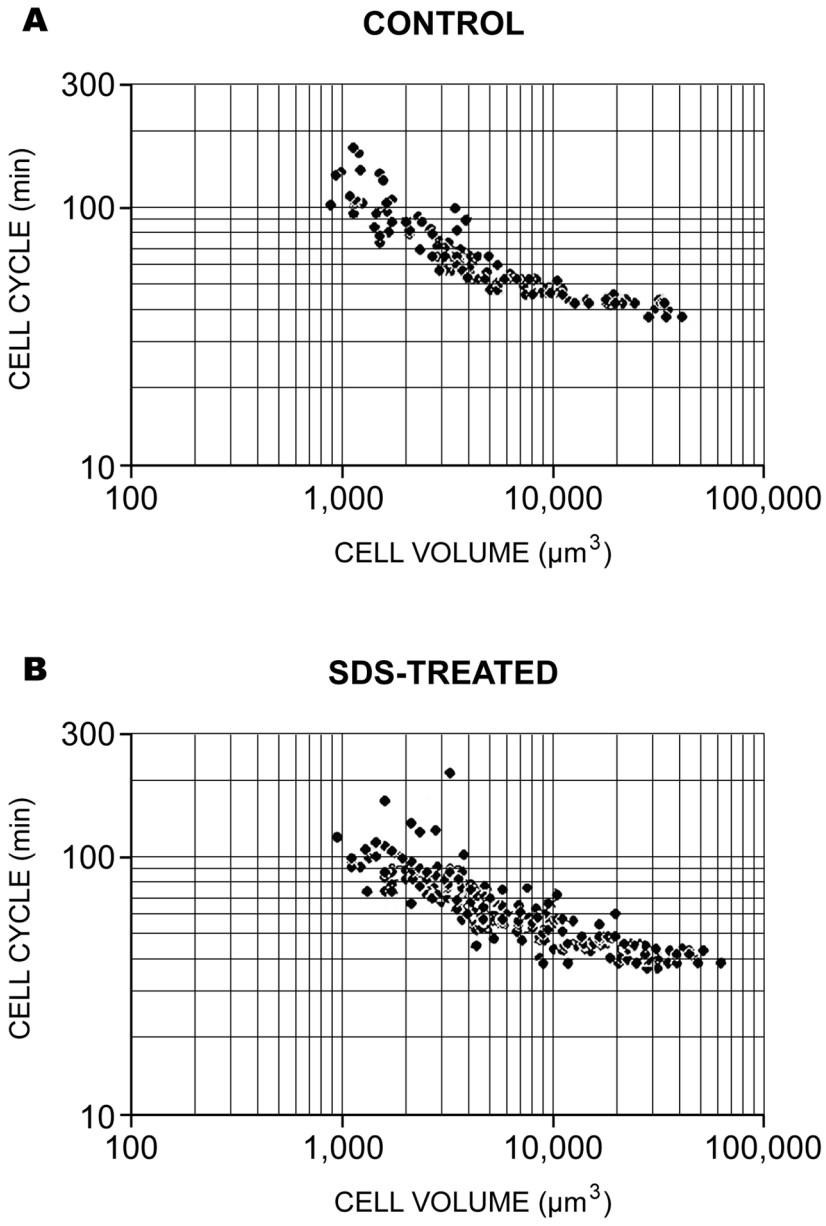

Figure 7.
The relationship between cell volume and cell cycle obtained from the time-lapse video records of Table 1. The data from 3 control (a) and 3 surfactant-treated embryos (b) are shown in a log-log plot. The slopes of the two standard linear regression lines from these plot lines are indistinguishable statistically using a variation of Student's *t*-test (Zar, 1974).

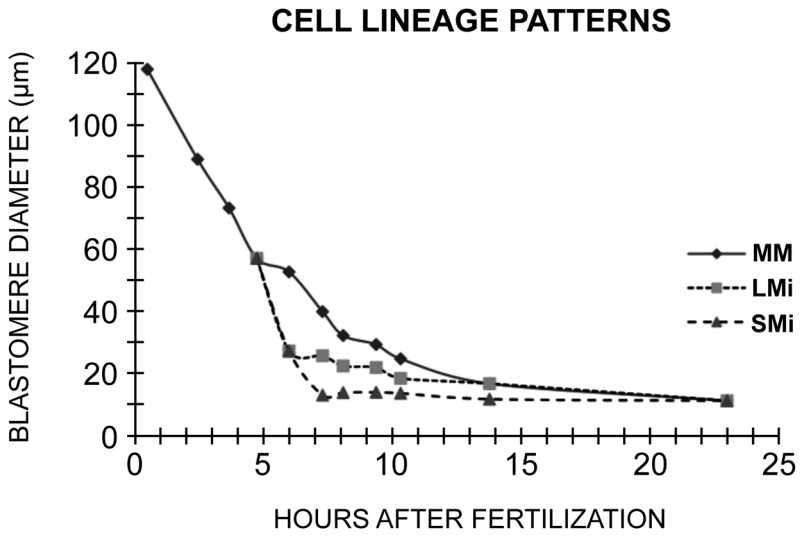

Figure 8.

Cell diameters as a function of cleavage stage in *Dendraster*. Embryos were dissociated and the blastomeres measured from photographs. One hundred cells were measured for each point. The lineages are indicated by MM (macro-mesomeres), LMi (large micromeres), and SMi (small micromeres), each lineage starting with its own cycle 1. Ciliation occurred at the 21st hour and hatching at 22.5 hours. The diameter achieved at hatching is 12 μm.

TABLE 1

	NORMAL EMBRYOS			SDS-TREATED EMBRYOS			
LINEAGE	**N**	**DIAMETER μm**	**CYCLE mins**	**LINEAGE**	**N**	**DIAMETER μm**	**CYCLE mins**
Small Micromeres							
SMi 1	10	15.9 ± 2.2	111.3 ± 32.9	“SMi 1”	10	29.2 ± 6.4	43.6 ± 4.80
SMi 2	2	14.2 ± 1.2	122.0 ± 2.6	“SMi 2”	23	22.1 ± 5.1	74.6 ± 40.3
SMi 3	0			“SMi 3”	26	19.9 ± 2.7	72.4 ± 21.2
SMi 4	0			“SMI 4”	19	14.9 ± 1.7	87.0 ± 11.7
Large Micromeres							
LMi 1	11	24.7 ± 3.4	46.1 ± 0.5	“LMi 1”	12	38.5 ± 6.6	39.9 ± 1.7
LMI 2	20	19.1 ± 1.6	58.3 ± 4.2	“LMi 2”	23	30.1 ± 4.0	45.5 ± 2.6
LMi 3	22	14.7 ± 1.9	88.7 ± 13.7	“LMi 3”	26	23.5 ± 4.5	56.2 ± 5.5
LMi 4	2	12.3 ± 0.2	133.5 ± 3.5	“LMi 4”	31	18.2 ± 3.2	78.1 ± 11.4
Macromeres							
MM 6	10	39.5 ± 2.3	39.8 ± 2.4	MM 6	13	40.4 ± 3.9	39.1 ± 2.3
MM 7	16	32.7 ± 2.2	42.6 ± 0.9	MM 7	14	33.1 ± 2.6	45.1 ± 1.2
MM 8	15	23.1 ± 1.7	50.5 ± 1.8	MM 8	10	25.5 ± 3.8	58.1 ± 4.3
MM 9	15	18.9 ± 1.1	66.1 ± 6.7	MM 9	12	19.3 ± 1.5	68.8 ± 4.1